ELSEVIER

Chemical Engineering Journal 140 (2008) 352–357

Chemical Engineering Journal

www.elsevier.com/locate/cej

Studying the internal mass transfer phenomena inside a Ni/Al_2O_3 catalyst for benzene hydrogenation

Kostas C. Metaxas, Nikos G. Papayannakos *

National Technical University of Athens, School of Chemical Engineering, Heroon Polytechniou 9, Zografos, 157 80 Athens, Greece

Received 20 February 2007; received in revised form 10 October 2007; accepted 11 October 2007

Abstract

The mass transfer phenomena occurring inside Ni/Al_2O_3 catalytic extrudates have been studied for the liquid-phase hydrogenation of benzene. The experiments were conducted in a bench scale trickle-bed reactor at 17 bar absolute pressure and temperatures between 70 and 150 °C. Kinetic, thermodynamic and hydrodynamic effects have previously been examined [K.C. Metaxas, N.G. Papayannakos, Ind. Eng. Chem. Res. 45(21) (2006) 7110–7119]. Temperature gradients inside the particle and across the liquid film surrounding catalyst particles have been checked and verified as absent. Concentration profiles of hydrogen and benzene show firstly that are consumed close to the surface of the extrudate and secondly to be in large excess along the particle radius. Catalyst particle tortuosity is estimated to be 3.75, very close to the value of 3.56 extracted from a statistical model based on nitrogen sorption hysteresis data. The effectiveness factor lies in the range of 0.19–0.35, implying strong diffusion limitations. The passivation of catalyst surface is posed as a solid reason for the modification of the true activation energy of the reaction occurred while moving from crushed catalyst particles to catalytic extrudates.

Keywords: Benzene hydrogenation; Intraparticle mass transfer; Effectiveness factor; Tortuosity; Catalyst extrudates

1. Introduction

Benzene hydrogenation is a well-known reaction that is enlisted in the general category of aromatics hydrogenation. Benzene hydrogenation is also a popular reaction because of its use for the production of cyclohexane – an intermediate of the industrial nylon process – and for decreasing benzene content in gasoline in accordance with the stricter legislation established in the year 2000. The gas-phase reaction has been widely studied, while few researchers have examined the liquid-phase reaction [2–6]. Studying the kinetics and mechanism of the reaction is mostly the case, but sometimes the main interest concerns catalyst characterization or mass transfer phenomena and hydrodynamics taking place inside a three-phase reactor.

The industrial reactor catalytic beds are constituted from particles around 0.15 cm in diameter. Smaller particles would create problems such as high pressure drop along the bed or hot spots in the catalyst bed and fast deactivation of the catalyst surface due to their high activity. To mimic industrial reactor's performance for scale up purposes, particles of the same size as that of industrial catalysts have been used in the laboratory experiments of this study, the main drawback of which is the pore diffusion resistance (intraparticle mass transfer limitations).

There are a number of studies that encounter the problem of internal concentration gradients inside a catalytic particle and estimate the corresponding effectiveness factor. Other researchers just avoid these gradients by crushing the catalyst in smaller particles till no more differences in reactant conversion can be observed. Few are the studies referring to trickle-bed reactors because of the coupling of several phenomena, which mask one another.

By conducting gas-phase benzene hydrogenation on two catalysts of different sizes (diameters of 0.45 cm and 0.05–0.063 cm), Jiracek et al. [7] tried to experimentally verify the theory of diffusion resistance and extract the effective diffusion coefficient of benzene. Toppinen et al. [4] solved the mass and energy balances that correspond to hydrogen–toluene diffusion and heat transfer inside a commercial Ni-Alumina catalyst on which liquid-phase hydrogenation of toluene takes place at 120 °C. They found negligible heat transfer limitation [$(\Delta T_{int})_{max} = 0.4$ °C], while hydrogen mass transfer controls the whole process, specially for toluene concentrations higher than

* Corresponding author. Tel.: +30 210 772 3239; fax: +30 210 772 3155.
E-mail address: npap@central.ntua.gr (N.G. Papayannakos).

1385-8947/$ – see front matter © 2007 Elsevier B.V. All rights reserved.
doi:10.1016/j.cej.2007.10.010

Nomenclature

A	cross section area of the reactor (cm^2)
a	volumetric interfacial area (cm^2/cm^3)
C_i	concentration of component i (concentration units e.g. mol/cm^3)
C_{Li}	concentration of component i (benzene or H_2) in liquid phase (mol/cm^3)
C_s	concentration of component i on the surface (concentration units e.g. mol/cm^3)
De_i	effective diffusivity of component i (benzene or H_2) (cm^2/s)
D_{Gi}	diffusion coefficient of component i (benzene or H_2) in gas phase (cm^2/s)
D_{Li}, D_i	diffusion coefficient of component i (benzene or H_2) in liquid phase (cm^2/s)
H_i	Henry constant of component i (benzene or H_2) ($bar/mol/cm^3$)
k_{Gi}	gas side mass transfer coefficient of component i (benzene or H_2) (s^{-1})
k_{GLi}	overall mass transfer coefficient of component i (benzene or H_2) (s^{-1})
k_{Li}	liquid side mass transfer coefficient of component i (benzene or H_2) (s^{-1})
ℓ_G or ℓ_L	film thickness in gas or liquid phase, respectively (cm)
N_{GLi}	gas–liquid mass transfer flux of component i (benzene or H_2) (mol/h)
N_{Li}	molar feed of component i (benzene or H_2) in liquid phase (mol/h)
N_{Vi}	molar feed of component i (benzene or H_2) in vapor phase (mol/h)
P_i	partial pressure of component i (benzene or H_2) (bar)
r	catalytic particle's radius (cm)
R	gas constant ($R = 8.31439 \pm 0.00034$ abs joule/deg mol)
r_p	reaction rate ($mol/h/g_{cat}$)
T	temperature (K)
$U_{g\ aver}$	average superficial gas-phase velocity (cm/s)
z	reactor length (cm)

Greek letters

ε	catalyst porosity
ρ_{bed}	catalytic bed density (g/cm^3)
τ	catalyst tortuosity

Subscripts

aver	average value
G or g	gas
I	benzene or hydrogen
L or l	liquid
V	vapor

5 wt.% (below this value toluene concentration becomes important too). Recently, Aumo et al. [8] studied the effect of pore diffusion for citral hydrogenation, when performed over trilobic Ni/Al_2O_3 catalyst in a semi-batch reactor.

Another point that has earned much of researchers' attention is the existence of thermal gradients inside the catalytic particle. These could deteriorate the reactor's performance, because of the reduced heat removal as phase transition takes place, which results in the formation of hot spots, appearance of multiple steady states [9] and hysteresis phenomena [10] or even reactor runaway [11—pellet reactor]. From the other hand, if this transition could be controlled, reactor performance would be intensified due to the increased diffusion rate by passing from the liquid to the gas region [12,13].

Kehoe and Butt [14] showed experimentally, that by conducting the gas-phase hydrogenation of benzene in a pellet-reactor, strong thermal effects exist at the boundary layer near the surface and inside the catalyst. By using particles of the same size but different thermal conductivity they observed a temperature rise with benzene concentration increase or gas flow reduction, only for the particles with low thermal conductivity. When reaction takes place in the liquid-phase, implying fully wetted catalyst, those thermal gradients are usually eliminated from the high thermal capacity of the surrounding liquid. Nevertheless, the validity of this assumption should be checked with some well-known criteria such as that of Prater, which allows the estimation of the maximum ΔT inside the catalytic particle.

Radial activity distribution, which in some cases improves reaction's yield or selectivity, has also been studied by few researchers. The optimal catalyst activity distribution was theoretically found to be, from the early 80 s already, a Dirac delta function [15]. Au et al. [16] studied gas-phase hydrogenation of benzene in a single pellet reactor using different distributions of Ni on the support. They concluded that for low effectiveness factor and high temperature, the catalyst with Ni-metal distributed primarily near the surface clearly exhibits the highest activity.

Sometimes, passivation of the catalyst is required due to one of the following reasons:

1. Its reduction cannot take place in the industrial reactor because of the high temperatures required or the lack of careful control of the process.
2. Its high activity needs to be protected during transportation, storage or reactor loading.
3. The catalyst is pyrophoric.
4. It could react with a common gas (e.g. CO) to produce toxic gases (e.g. $Ni(CO)_4$).

The passivation usually takes place by slowly supplying O_2 to the catalyst (in some cases CO or CO/H_2 are preferred) to form a layer of oxides on the surface and so reduce its activity. Menon and Skaugset [17] underline the matter of passivated catalyst crushing, which could result in alteration of its activity, as not passivated surface would be exposed to air and hence re-oxidized.

In this work, benzene hydrogenation is used as a model reaction in order to study the intraparticle mass transfer limitations

inside industrial catalytic particles operating in a trickle bed reactor. The final task is to obtain the concentration profiles of reactants along the particle radius, to evaluate the effect of each reactant's concentration profile on the particle effectiveness factor and to estimate the tortuosity of the catalytic particles.

2. Experimental

The reaction of liquid-phase benzene hydrogenation to cyclohexane was studied in a bench-scale reactor (2.54cm in diameter, 47.5 cm in length). The range of temperatures used is 70–150 °C, the absolute pressure is 17 bar, the concentration of benzene at the inlet lies between 2.7 and 4.1 wt.%, the maximum conversion of benzene is 97% and the minimum 38%, the mass liquid flow rate ranges from 60 to 120 g/h, the volumetric gas flow rate is 3–6 l/h and the weighted hourly space velocity (WHSV) varies between 9 and 18 h^{-1}. 6.7 g of commercial trilobe nickel on alumina catalytic extrudates were diluted with 100 g of non-porous diluent (Carborundum-SiC, 0.025 cm in diameter) to build a diluted catalytic bed 12.2 cm in length. The solvent used is a mixture of *n*-hexane and cyclohexane (concentrations up to 30 wt.% regarding cyclohexane). More details of the operating conditions are given in a previous publication [1].

Catalyst porosity was measured using Hg and He porosimetry and was found equal to 0.46, while its density is 2.7 g/cm^3. N_2 porosimetry produces common hysterisis curves for adsorption–desorption data and one-peak pore distribution for the catalyst considered, as shown in Fig. 1. The average pore diameter is 94 Å. By using electron microscope scanning and X-ray analysis of the surface (SEM-EDAX), the uniform distribution of Nickel on Alumina substrate was verified.

3. Mathematical model

A detailed mathematical model incorporating liquid volatility (Soave-Redlich-Kwong cubic equation of state [18]) and inter- and intra-particle mass transfer effects has been developed in order to describe reactor's behavior [1]. The following mass balances for the reactants being in the liquid and vapor phase respectively, are adopted:

$$\frac{dN_{L_B}}{dz} = aN_{GLB} - r_p\rho_{bed}A = \left[k_{GL_B}a\left(\frac{P_B}{H_B} - C_{L_B}\right) - r_p\rho_{bed}\right]A \quad (1)$$

$$\frac{dN_{L_H}}{dz} = aN_{GLH} - 3r_p\rho_{bed}A = \left[k_{GL_H}a\left(\frac{P_H}{H_H} - C_{L_H}\right) - 3r_p\rho_{bed}\right]A \quad (2)$$

$$\frac{dN_{V_B}}{dz} = k_{GL_B}a\left(\frac{P_B}{H_B} - C_{L_B}\right)A \quad (3)$$

$$\frac{dN_{V_H}}{dz} = k_{GL_H}a\left(\frac{P_H}{H_H} - C_{L_H}\right)A \quad (4)$$

The overall gas–liquid mass transfer coefficient is related to the gas- and liquid-side mass transfer coefficients and the Henry constant in the following manner:

$$k_{GL_i} = \frac{1}{1/k_{L_i} + 1/k_{G_i}H_i^*} = \frac{1}{1/k_{L_i} + RT/k_{G_i}H_i} \quad (5)$$

The gas- and liquid-side mass transfer coefficients are connected to the film thicknesses (ℓ_G or ℓ_L) and diffusion coefficients (D_{Gi} or D_{Li}) of the gas and liquid phase through the relations:

$$k_{Li} = \frac{D_{Li}}{\ell} \Rightarrow ak_{Li} = D_{Li}\frac{a}{\ell}\Big|_L \Rightarrow \frac{a}{\ell}\Big|_L = \frac{ak_{Li}}{D_{Li}} \quad (6)$$

$$k_{Gi} = \frac{D_{Gi}}{\ell_G} \Rightarrow ak_{Gi} = D_{Gi}\frac{a}{\ell}\Big|_G \Rightarrow \frac{a}{\ell}\Big|_G = \frac{ak_{Gi}}{D_{Gi}} \quad (7)$$

The proposed correlations extracted for the gas- and liquid-side mass transfer coefficients when working in the same range of velocities, in the same reactor, with a diluted bed of the same diluent as the one used in this work but on crushed particles of Ni/Al_2O_3 are the followings [1]:

$$\ln\left(\frac{ak_{Li}}{D_{Li}}\right) = 1.17\ \ln(U_{g\,aver}) + 9.32 \quad (8)$$

$$\ln\left(\frac{ak_{Gi}}{D_{Gi}}\right) = 2.52\ \ln(U_{g\,aver}) + 9.40 \quad (9)$$

The reaction rates of hydrogenation in Eqs. (1) and (2) were calculated by using the liquid concentration profiles of benzene and hydrogen inside the catalyst extrudates. These profiles were determined by solving the following second order ordinary differential equation of diffusion-reaction for each component.

$$\frac{d^2C_i}{dr^2} + \frac{1}{r}\frac{dC_i}{dr} - \frac{r_p}{De_i} = 0 \quad (10)$$

where C_i is the concentration of component i, r is the particle's radius, r_p is the reaction rate and De_i is the effective diffusivity. In this case, we have reduced the shape of the trilobe particles to a cylindrical form with the same particle volume to external

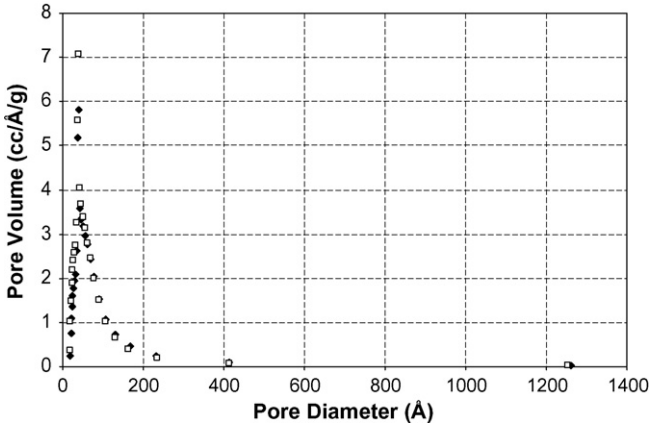

Fig. 1. The distribution of pore volume versus pore diameter extracted from nitrogen porosimetry. (□): Crushed particles, (♦): extrudates.

surface ratio. The effective diffusivity depends on particle's and fluid's properties according to the following relation:

$$\mathrm{De}_i = \frac{\varepsilon}{\tau} D_i \tag{11}$$

where ε is particle's porosity, τ is particle's tortuosity and D_i is the diffusion coefficient of the reactant i in the fluid inside he catalyst pores. To solve the differential equation, two boundary conditions are needed:

$$\begin{aligned} r = 0 \quad & \frac{\mathrm{d}C_i}{\mathrm{d}r} = 0 \\ r = R \quad & C_i = C_\mathrm{s} \end{aligned} \tag{12}$$

The first is valid at the center of the catalytic particle and indicates the symmetry of space in that dimension and the lack of concentration gradient at this point, while the second corresponds to particle's surface.

The differential equations for the two reactants inside the catalyst particles are solved with finite difference approximation while the system of non-linear equations produced is solved with a modified Powell hybrid algorithm. Matrixes of 10, 50, 100, 1000 nodes were tested with augmentative impact on computer time needed for the solution to be accomplished. By assuming minimal error when using a matrix of 1000 nodes, the matrixes of 50 and 100 nodes were compared (that with the 10 nodes failed to produce meaningful results), with the first achieving 2.5% accuracy and the second 1.1% but double computer time. Finally the 50-node matrix was preferred as this accuracy was in the range of the experimental error and because of the large volume of experimental data that make computer time precious.

4. Results and discussion

For the simulation of the laboratory reactor performance with the previously described model, the intrinsic kinetic form as well as the inter-particle mass transfer effects have been adopted from a recent publication [1]. In both works, identical hydrodynamic characteristics for the two systems are expected as the same diluent was used for the building of the relevant diluted catalyst beds [19].

Although between 70 and 150 °C, a significant amount of the liquid mixture at the reactor inlet is vaporized (13–33 vol% depending also on gas to liquid velocities), the dilution of the catalyst bed with fine particles (SiC) ensures the full wetting of catalyst particles [20–22] and the avoidance of liquid maldistribution or axial dispersion [22–24,25—review].

Before solving the diffusion equations, we had to ensure that the catalytic particles work isothermally. Due to the fully wetting of the particle, the diffusion coefficients of benzene and hydrogen refer to the liquid phase. Characteristic values for the thermal conductivity coefficient of Ni/Al_2O_3 are given by Satterfield [26]. The maximum ΔT inside the catalyst particles is easily calculated [27] and it was found less than 0.05 °C for the worst case of reaction temperature $T = 150$ °C. Therefore, no internal temperature gradients exist in our range of operational conditions. Using the modified Sherwood and Nusselt numbers–appropriate values for heat transfer and thermal conductivity coefficients in the liquid are found in Perry's Chemical Engineers' Handbook [28]–the maximum ΔT appearing at the external liquid film that surrounds the catalytic particle can also be evaluated. The temperature gradient in the liquid film surrounding the catalyst external surface was also proved to be negligible [$(\Delta T_{\mathrm{ext}})_{\max} = 0.14$ °C].

When fitting the experimental data into simulation predictions, it was proved that the intrinsic kinetics, having been obtained from crushed particles, had to be modified as the predicted hydrogenation rates were higher than the experimentally measured ones. The only change needed was the modification of the values of the reaction rate constants. Utilizing a unique tortuosity value for all experimental data, the intrinsic reaction rate constant was estimated for each experimental set performed at the same temperature. This was attained by best fitting the predicted benzene concentrations at the reactor outlet into the corresponding experimental ones for all the experiments. The values of the reaction rate constant corresponding to the best fitting are presented in Fig. 2. The apparent activation energy calculated from the data of this figure is 103.7 kJ/mol corresponding to a true activation energy of 55 kJ/mol. The comparison of the predicted with the experimental values of benzene conversion for all the data is presented in Fig. 3, where a good agreement is observed.

A different behavior of the crushed catalyst particles than that of the mother extrudates was also observed when activity loss with time was studied. As shown in Fig. 4, the deactivation rate with the crushed particles was much faster than the corresponding with the extrudates when pure n-hexane was used as solvent. The same tendency was observed when an industrial feed was tested, although for both catalyst sizes the decline was faster. The different deactivation rates and the different intrinsic reaction rate constants estimated for the crushed particles and the mother extrudates can be explained by a partial passivation of the extrudates near the external surface of the catalyst. Thus, the part of the catalyst close to the external surface has lower activity and deactivates much slower than the internal part. In the sample of the crushed extrudates, the entire catalyst surface partakes of the hydrogenation reaction and the fast deactivation is

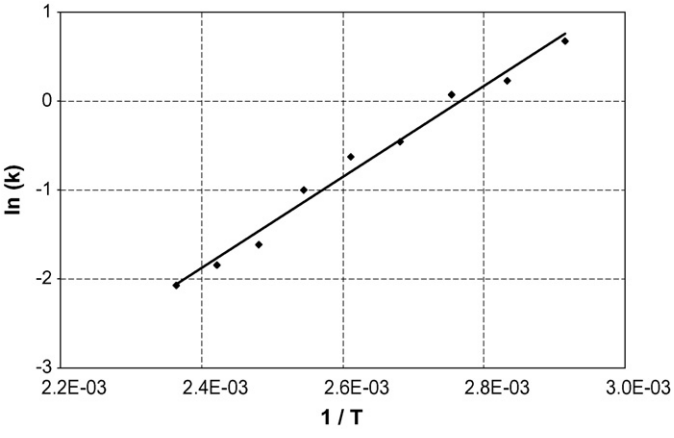

Fig. 2. The dependence of the determined reaction rate constant on reaction temperature.

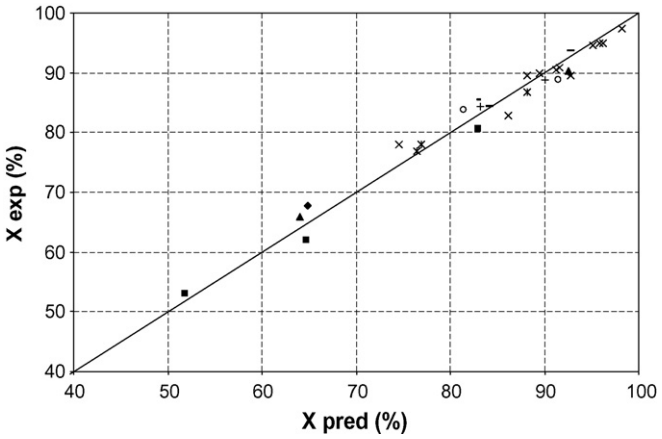

Fig. 3. Comparison of the predicted conversions (X_{pred}) with the corresponding experimental values (X_{exp}) at various reaction temperatures from 70 to 150 °C. (♦)70, (■)80, (▲)90, (×)100, (✱)110, (◯)120, (+)130, (–)140, (▬)150.

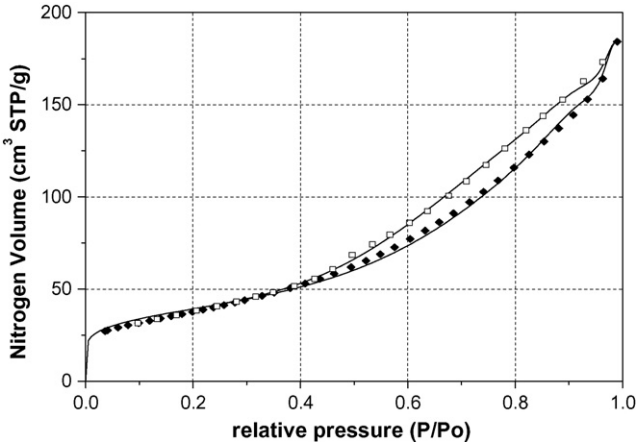

Fig. 5. Fitting of CPSM statistical model to nitrogen sorption hysteresis loop experimental data. (□): desorption, (♦): adsorption.

due to the particles from the interior of the extrudates that are not passivated and now are exposed to high benzene and hydrogen concentrations. Furthermore, because the reaction takes place close to the surface of the extrudates, as will be discussed in the followings, the intrinsic kinetics describing the hydrogenation rates in Eqs. (1) and (2) should correspond to this restricted area having lower activity. These rates are lower than those corresponding to the internal part of the catalyst extrudates due to passivation. Therefore, the intrinsic rates corresponding to this part are lower than the rates obtained from the crushed particles because in the latter case the high rates of the non-passivated internal parts would give rise to the mean rates of the sample.

The tortuosity determined from the optimization procedure was 3.75, a typical value of this kind of catalysts. There was also an attempt to compare the tortuosity extracted by the optimization method processing the experimental data with the approach of a stochastic model. In particular, Androutsopoulos and Salmas [29,30] have developed a statistical model (CPSM) that uses nitrogen sorption hysteresis data taken by applying N_2 porosimetry on fresh catalytic extrudates. Their model fits nitrogen adsorption–desorption data by optimizing tortuosity [31]. This method yields a value of 3.56 for the tortuosity of the extrudates, which is very close to the estimated value from our model (3.75). The fitting of the CPSM model over the experimental hysteresis loop data is presented in Fig. 5.

From the calculated profile of hydrogen concentration given in Fig. 6 it is observed that hydrogen is consumed in the first quarter of particle's radius (∼0.02 cm). On the contrary, benzene concentration decreases mostly by 20% along the particle radius being in excess inside the catalyst extrudates. Therefore, a small part of the extrudates is used for the hydrogenation of benzene due to the total consumption of hydrogen. The effectiveness factor of the extrudates is thus controlled by hydrogen diffusion and reaction. In Fig. 7, the calculated effectiveness factor for the extrudates is shown. It appears decreasing from 0.35 at 70 °C to 0.19 at 150 °C, implying strong diffusion limitations.

However, for the crushed particles a slight decrease of hydrogen (less than 35%) and benzene concentration (less than 20%) is calculated along the particle radius. The effectiveness factor calculated from the concentration profiles lies between 0.85 and 0.99 (70–100 °C, Thiele modulus less than 0.65), implying a restricted role of mass transfer resistances.

Toppinen et al. [4] found that for toluene concentrations above 5 wt.% hydrogen mass transfer controls the whole process,

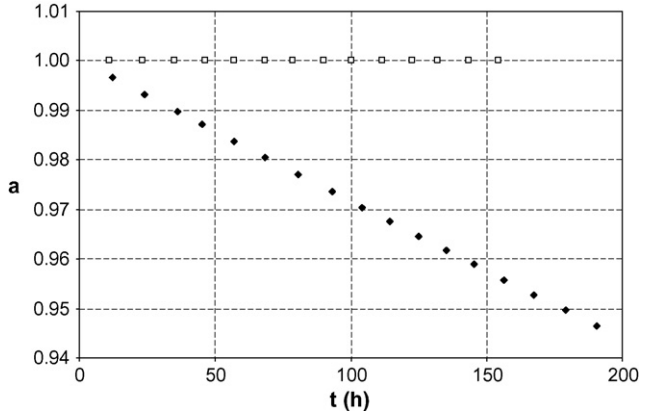

Fig. 4. The activity (a) of the crushed catalyst and of the extrudates versus working hours, with *n*-hexane as feed solvent. (□): Extrudates, (♦): crushed particles.

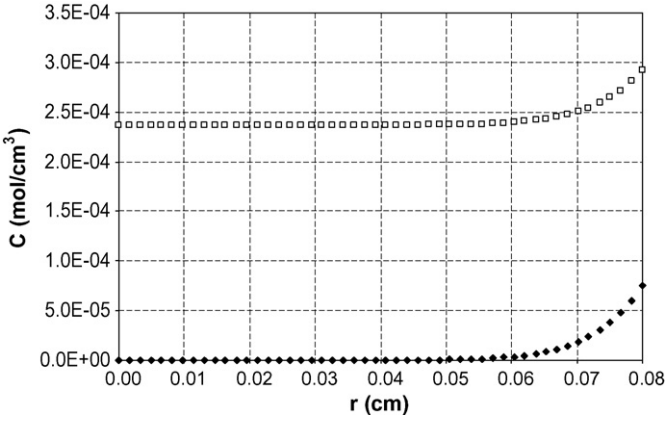

Fig. 6. Concentration profiles of hydrogen and benzene along the catalytic extrudate's radius. (□): Benzene, (♦): hydrogen.

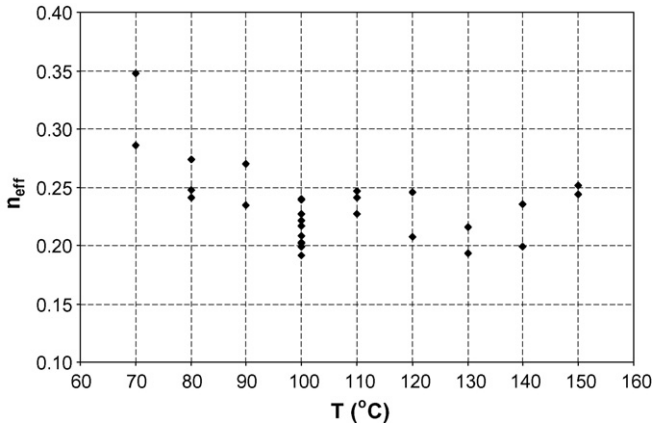

Fig. 7. The effectiveness factor calculated by optimizing catalyst's tortuosity for every one of the 29 experiments, versus temperature.

when working at 120 °C with extrudates loaded with 16.6 wt.% Ni on alumina substrate and of diameter of 0.1 cm. The concentration profiles of hydrogen and toluene show hydrogen to be almost totally consumed in the 3/4 of the catalytic particle (0.075 cm), while toluene's concentration remains constant. In our case, benzene concentration at the inlet of the reactor is about 4 wt.%, Ni-metal is above 50 wt.% on the alumina and benzene is hydrogenated faster than toluene [32]. This is why the decline of hydrogen concentration is more abrupt as it takes place in the 1/4 of particle's radius (0.02 cm) with benzene being in large excess throughout the particle.

Aumo et al. [8] worked with a less active catalyst (20.2 wt.% Ni) at lower temperatures (60 °C) which result in lower hydrogenation rates as compared to our case. Because of the low citral concentration the hydrogen was in excess inside the trilobic catalyst, while the citral was totally consumed in the first half of the catalytic particle. They come up with a catalyst's porosity to tortuosity ratio equal to 0.27 and an effectiveness factor close to 0.2 while in this work the respective values are: 0.16 and 0.23.

5. Conclusions

Summarizing, by processing experimental data extracted from the liquid-phase hydrogenation of benzene on Ni/Al_2O_3 extrudates in a trickle-bed reactor, the following tasks have been accomplished:

1. The concentration profiles of benzene and hydrogen inside the catalytic particle indicate that hydrogen is depleted in the first 25% of the particle radius while benzene is in excess throughout the catalyst particles.
2. The calculated effectiveness factor of the catalyst extrudates was less than 0.35 indicating strong diffusional limitations.
3. The tortuosity of the catalytic particle was estimated equal to 3.75 and found in good agreement with the value extracted from a statistical model (3.56).

The reaction kinetics of hydrogenation obtained from experiments with crushed particles had to be modified at the point of dependence of the reaction rate constant on reaction temperature and this inevitable change was attributed to catalyst's surface passivation.

Acknowledgements

We are obliged to Motor-Oil Hellas Refinery and the State Scholarships Foundation of Greece for the financial support of this work. We would like also to thank Dr. Salmas who conducted nitrogen porosimetry on our fresh catalytic extrudates and treated the experimental data with CPSM statistical model.

References

[1] K.C. Metaxas, N.G. Papayannakos, Ind. Eng. Chem. Res. 45 (21) (2006) 7110–7119.
[2] D.Yu. Murzin, N.A. Sokolova, N.V. Kul'kova, M.I. Temkin, Kinet. Katal. 30 (6) (1989) 1352–1358.
[3] D.S. Sharma, K. Gadgil, K.M. Sarkar, Chem. Eng. Technol. 16 (1993) 347–359.
[4] S. Toppinen, T.K. Rantakyla, T. Salmi, J. Aittamaa, Ind. Eng. Chem. Res. 35 (1996) 1824–1833.
[5] J. Franco, S. Marzuka, J. Papa, J.T. de Herrera, Recents Progres en Genie des Procedes 13 (65) (1999) 123–130.
[6] U.K. Singh, M.A. Vannice, AIChE J. 45 (5) (1999) 1059–1071.
[7] F. Jiracek, J. Horak, J. Pasek, AIChE J. 15 (3) (1969) 400–404.
[8] J. Aumo, J. Warna, T. Salmi, Y.D. Murzin, Chem. Eng. Sci. 61 (2006) 814–822.
[9] V.A. Kirillov, I.V. Koptyug, Ind. Eng. Chem. Res. 44 (2005) 9727–9738.
[10] R. Maiti, R. Khanna, K.D.P. Nigam, Ind. Eng. Chem. Res. 45 (15) (2006) 5185–5198.
[11] P.C. Watson, M.P. Harold, AIChE J. 39 (6) (1993) 989–1006.
[12] Z.-M. Cheng, A.M. Anter, W.-K. Yuan, AIChE J. 47 (5) (2001) 1185–1192.
[13] L.B. Datsevich, Appl. Catal. A 279 (2005) 18–185.
[14] J.P.G. Kehoe, J.B. Butt, AIChE J. 18 (2) (1972) 347–355.
[15] M. Morbidelli, A. Servida, A. Varma, Ind. Eng. Chem. Fundam. 21 (1982) 278.
[16] S.S. Au, J.S. Dranoff, J.B. Butt, Chem. Eng. Sci. 50 (23) (1995) 3801–3812.
[17] P.G. Menon, P. Skaugset, Appl. Catal. A: Gen. 115 (1994) 295–302.
[18] M.S. Graboski, T.E. Daubert, Ind. Eng. Chem. Process Des. Dev. 17 (1978) 443.
[19] M.H. Al-Dahhan, F. Larachi, M.P. Dudukovic, A. Laurent, Ind. Eng. Chem. Res. 36 (1997) 3292–3314.
[20] J. van Klinken, R.H. van Dongen, Chem. Eng. Sci. 35 (1980) 59–66.
[21] D.C. Tsamatsoulis, N.G. Papayannakos, AIChE J. 42 (7) (1996) 1853–1863.
[22] M.H. Al-Dahhan, M.P. Dudukovic, AIChE J. 42 (9) (1996) 2594–2606.
[23] D.C. Tsamatsoulis, N.G. Papayannakos, Chem. Eng. Sci. 49 (4) (1994) 523–529.
[24] A. Chander, A. Kundu, S.K. Bej, A.K. Dalai, D.K. Vohra, Fuel 80 (2001) 1043–1053.
[25] S.K. Bej, Energy Fuels 16 (2002) 774–784.
[26] C.N., Satterfield, Mass Transfer in Heterogeneous Catalysis, Robert E. Krieger, 1981.
[27] G.F. Froment, K.B. Bischoff, Chemical Reactor Analysis and Design, John Wiley & Sons, 1979.
[28] Perry's Chemical Engineers' Handbook, McGraw-Hill, seventh ed., 1999.
[29] G.P. Androutsopoulos, C.E. Salmas, Ind. Eng. Chem. Res. 39 (2000) 3747–3763.
[30] G.P. Androutsopoulos, C.E. Salmas, Ind. Eng. Chem. Res. 39 (2000) 3764–3777.
[31] C.E. Salmas, G.P. Androutsopoulos, Ind. Eng. Chem. Res. 40 (2) (2001) 721.
[32] D. Poondi, M.A. Vannice, J. Catal. 161 (1996) 742–751.